

927,258,1986)]. The resulting mixture was used to transform *Escherichia coli* strain HB101 cells, and a plasmid encoding 36 repeats of sequence **1a** was selected for further characterization. The target DNA was subcloned in pET3-b to yield pET3bMK36, an expression vector in which transcription is driven by bacteriophage T7 RNA polymerase (38). In this construction, the target protein sequence is flanked by plasmid-derived amino- and carboxyl-terminal extensions of 23 and 32 residues, respectively (sequence **3**). The host used for protein expression was *E. coli* strain BL21(DE3) pLysS, which carries a gene encoding T7 RNA polymerase incorporated into the bacterial chromosome under *lacUV5* control. This configuration allows protein production to be induced by isopropyl β -D-galactopyranoside (IPTG). The ancillary plasmid pLysS provides a low-level source of T7 lysozyme, which inhibits T7 RNA polymerase and suppresses the basal level of protein expression (38).

13. K. P. McGrath, M. J. Fournier, T. L. Mason, D. A. Tirrell, *J. Am. Chem. Soc.* **114**, 727 (1992).
14. Abbreviations for the amino acid residues are as follows: A, Ala; C, Cys; D, Asp; E, Glu; F, Phe; G, Gly; H, His; I, Ile; K, Lys; L, Leu; M, Met; N, Asn; P, Pro; Q, Gln; R, Arg; S, Ser; T, Thr; V, Val; W, Trp; and Y, Tyr.
15. B. J. Smith, *Methods in Molecular Biology: New Protein Techniques* (Humana, Totowa, NJ, 1988), p. 70.
16. The structure of the cleaved protein product was confirmed by ^1H NMR spectroscopy, amino acid analysis, and combustion analysis. Calculated amino acid analysis (mol percent): Ala, 37.4; Glx, 12.3; Gly, 49.7. Values found: Ala, 35.6; Glx, 13.1; Gly, 49.3. Calculated combustion analysis (percent by weight; including 2.5% H_2O by weight): C, 45.1; H, 6.2; N, 19.2. Values found: C, 46.1; H, 6.2; N, 18.0. Typical isolated yields of **3** corresponded to ~25% of total cellular protein. Thermogravimetric analysis in air revealed an onset of degradation at 235°C. No thermal transitions were evident by differential scanning calorimetry from room temperature to 235°C.
17. R. D. B. Fraser, T. P. MacRae, F. H. C. Stewart, E. Suzuki, *J. Mol. Biol.* **11**, 706 (1965).
18. W. H. Moore and S. Krimm, *Biopolymers* **15**, 2483 (1976).
19. T. Miyazawa and E. R. Blout, *J. Am. Chem. Soc.* **83**, 712 (1961).
20. S. Krimm and J. Bandekar, *Adv. Protein Chem.* **38**, 181 (1968).
21. B. G. Frushour and J. L. Koenig, *Biopolymers* **14**, 2115 (1975).
22. B. G. Frushour, P. C. Painter, J. L. Koenig, *J. Macromol. Sci. Rev. Macromol. Chem. C* **15**, 29 (1976).
23. The CP/MAS ^{13}C NMR spectra of **1a** were obtained at 50.6 MHz on powder samples with the use of a Bruker AC 200 spectrometer equipped with a DOTY solids probe and an IBM solids rack. Measurements were collected at a spinning speed of ~4000 Hz with a 5- μs 90° pulse and a cross polarization time of 2 ms. A line-broadening factor of 50 was applied during data processing. Chemical shifts were compared with those reported by H. Saito *et al.*, *Macromolecules* **17**, 1405 (1984).
24. M. Ishida, T. Asakura, M. Yokoi, H. Saito, *Macromolecules* **23**, 88 (1990).
25. J. O. Warwicker, *J. Mol. Biol.* **2**, 350 (1960).
26. L. Brown and I. F. Trotter, *Trans. Faraday Soc.* **52**, 537 (1956).
27. A. Keller, *J. Polym. Sci.* **36**, 361 (1959); E. D. T. Atkins *et al.*, *J. Polym. Sci. A* **2**, 863 (1972); P. Dreyfuss and A. Keller, *J. Polym. Sci. B* **8**, 253 (1970); J. H. Magill *et al.*, *Polymer* **22**, 43 (1981).
28. G. Hirschsen, *Makromol. Chem.* **166**, 291 (1973).
29. F. Lucas *et al.*, *J. Mol. Biol.* **2**, 339 (1960).
30. G. Nemethy and M. P. Printz, *Macromolecules* **5**, 755 (1972).
31. K. Sakaoku, N. Morosoff, A. Peterlin, *J. Polym. Sci. Polym. Phys. Ed.* **11**, 31 (1973).
32. C. G. Vonk, in *Small Angle X-ray Scattering*, O. Glatzer and O. Kratky, Eds. (Academic Press, New York, 1982), p. 443.
33. M. T. Krejchi, E. D. T. Atkins, M. J. Fournier, T. L.

Mason, D. A. Tirrell, unpublished results.

34. D. C. Bassett, *Morphology of Polymers* (Cambridge Univ. Press, Cambridge, 1981).
35. We have recently completed a spectroscopic study of the related polypeptide **4**, which provides persuasive direct evidence for adjacent reentry folding

$$\text{---}[(\text{AlaGly})_3\text{GluGly}(\text{GlyAla})_3\text{GluGly}]\text{---}$$
 [A. Parkhe, M. J. Fournier, T. L. Mason, D. A. Tirrell, *Macromolecules* **26**, 6691 (1993)].
36. R. E. Marsh, R. B. Corey, L. Pauling, *Biochim. Biophys. Acta* **16**, 1 (1955).
37. F. W. Studier, A. H. Rosenberg, J. J. Dunn, *Methods Enzymol.* **185**, 60 (1990).
38. Media were prepared according to J. Sambrook,

E. F. Fritsch, T. Maniatis, *Molecular Cloning: A Laboratory Manual* (Cold Spring Harbor Laboratory Press, Cold Spring Harbor, NY, ed. 2, 1989), p. A. 3.

39. We thank J. Cappello for the gift of p937.51 and for helpful advice, S. L. Hsu for guidance in vibrational spectroscopy, and L. K. Thompson for help in obtaining solid-state NMR spectra. Y. Deguchi developed methods for the preparation of polymers **1b** through **1d**. We are grateful to A. D. Parkhe for preparing Fig. 2 and to S. Cooper for Fig. 8. Supported by grants from the Polymers and Genetics Programs of the National Science Foundation (NSF) and by the NSF Materials Research Laboratory at the University of Massachusetts.

4 April 1994; accepted 7 July 1994

Stress Triggering of the 1994 $M = 6.7$ Northridge, California, Earthquake by Its Predecessors

Ross S. Stein, Geoffrey C. P. King, Jian Lin

A model of stress transfer implies that earthquakes in 1933 and 1952 increased the Coulomb stress toward failure at the site of the 1971 San Fernando earthquake. The 1971 earthquake in turn raised stress and produced aftershocks at the site of the 1987 Whittier Narrows and 1994 Northridge ruptures. The Northridge main shock raised stress in areas where its aftershocks and surface faulting occurred. Together, the earthquakes with moment magnitude $M \geq 6$ near Los Angeles since 1933 have stressed parts of the Oak Ridge, Sierra Madre, Santa Monica Mountains, Elysian Park, and Newport-Inglewood faults by more than 1 bar. Although too small to cause earthquakes, these stress changes can trigger events if the crust is already near failure or advance future earthquake occurrence if it is not.

The 17 January 1994 Northridge earthquake was the most costly shock in the history of the United States, underscoring the vulnerability of urban areas to earthquakes. The event struck on a blind or buried thrust fault (1) inclined to the south. The 1971 $M = 6.7$ San Fernando earthquake struck on adjacent thrust faults inclined to the north (2). Both earthquakes were responses to crustal compression across the greater Los Angeles area. Not only did aftershocks of the San Fernando (3) and Northridge (4) earthquakes spatially overlap (Fig. 1), but the 23-year span between the events is small relative to their probable thousand-year repeat times (5), suggesting that the two shocks are related. Here we argue that the San Fernando shock increased stress at the future Northridge rupture zone by up to 2 bars, potentially advancing its occurrence by two decades. This hypothesis is supported by the observation that aftershocks of the 1971 and 1994 earthquakes were concentrated where the stresses are calculated to have risen, and

aftershocks were sparse where the stresses are calculated to have dropped.

We calculate the Coulomb stress change caused by one earthquake on the rupture surface of a subsequent shock or

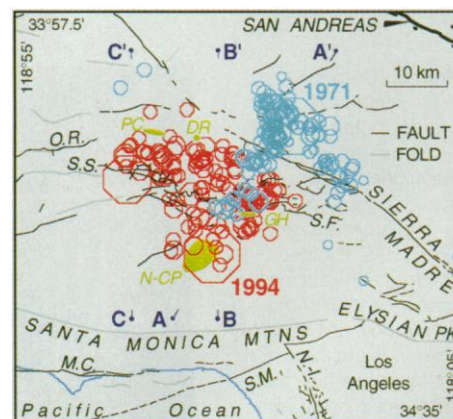


Fig. 1. Overlapping aftershocks of the 1971 San Fernando (blue; first year, $M \geq 2$) and 1994 Northridge (red; first 24 days, $M \geq 3$) earthquakes. Sites of mapped secondary surface faulting or cracked ground (green) (19): N-CP, Northridge-Canoga Park; GH, Granada Hills; PC, Potrero Canyon; DR, Davidson Ranch. Faults: O.R., Oak Ridge; S.S., Santa Susana; S.F., San Fernando; M.C., Malibu Coast; S.M., Santa Monica; N.-I., Newport-Inglewood. Cross-section orientations of Fig. 3 are also shown.

R. S. Stein, U.S. Geological Survey, Mail Stop 977, Menlo Park, CA 94025, USA. E-mail: stein@andreas.wr.usgs.gov.
G. C. P. King, Institut de Physique du Globe, Strasbourg 67084, France. E-mail: king@klakmuf.u-strasbg.fr.
J. Lin, Woods Hole Oceanographic Institution, Woods Hole, MA 02543, USA. E-mail: jian@galileo.whoi.edu.

on a known fault (6). The tendency of rocks to fail in a brittle manner is thought to be a function of both shear and confining stresses, commonly formulated as the Coulomb criterion. The Coulomb stress change depends on the geometry and slip of the earthquake, the geometry and sense of slip of the fault or surface of interest, and the effective coefficient of friction (7–9). We used this method to

estimate how successive southern California earthquakes transferred stress.

We further developed a Coulomb criterion for small earthquakes or aftershocks. Because small shocks can occur on small isolated faults, which exist with a wide variety of orientations throughout the crust, the faults most likely to slip are those optimally oriented for failure as a result of the regional stress and the stress

change caused by a preceding earthquake (9, 10). Aftershocks of several strike-slip earthquakes (the 1979 Homestead Valley and the 1992 Joshua Tree, Landers, and Big Bear shocks) have occurred in regions where the stress change on optimally oriented vertical faults was increased by >0.3 bar, and their aftershocks were sparse where the stress dropped by the same amount (11). For this study, we

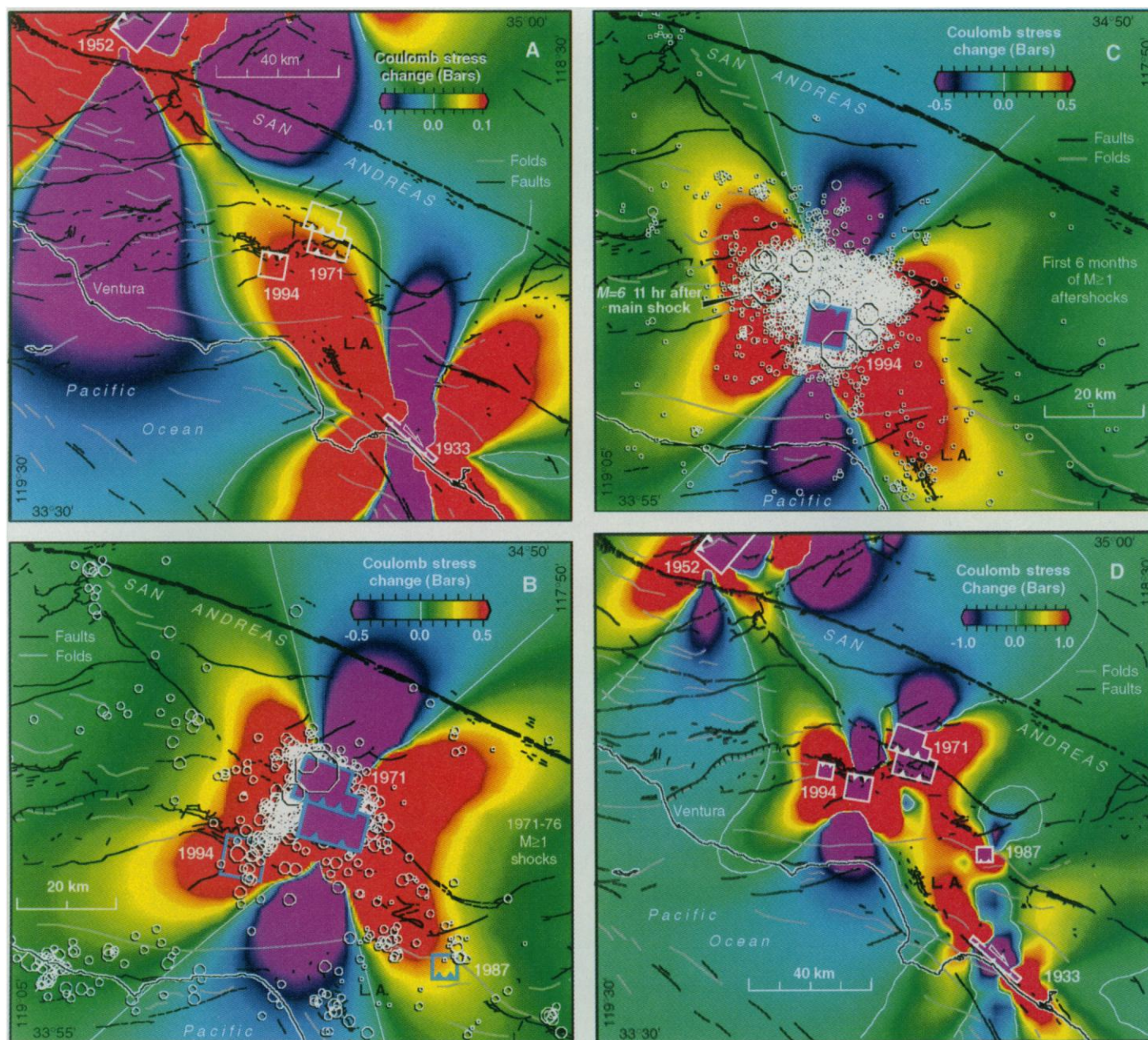


Fig. 2. Map views of calculated Coulomb stress changes on optimally oriented strike-slip or thrust faults in an elastic half-space for a regional stress direction of $N16^{\circ}E$ and a friction coefficient $\mu = 0.4$. Earthquakes that caused stress changes are denoted by purple-filled rectangles with teeth on the upper edge; future sources are unfilled rectangles. The color gradients representing stress change saturate below the calculated peak stress changes. The southern California coastline is a white-enclosed black line. L.A., Los Angeles. **(A)** Calculated stress change caused by the 1933 $M = 6.4$ Long Beach and 1952 $M = 7.3$ Kern County earthquakes, sampled at a depth of 10 km, showing sites of the future San

Fernando and Northridge earthquakes. **(B)** Stress changes caused by the 1971 $M = 6.7$ San Fernando earthquake. The most positive stress change at a depth of 3 to 10 km is shown, along with 5 years of post-earthquake $M \geq 1$ shocks [number of stations ≥ 4 , root-mean-square (rms) timing error ≤ 1 s]. **(C)** Stress changes caused by the 1994 $M = 6.7$ Northridge earthquake. The most positive stress change at a depth of 3 to 10 km is shown, along with $M \geq 1$ shocks during 17 January to 12 July 1994 (rms timing error ≤ 0.3 s). **(D)** Effect of all $M \geq 6$ shocks within 125 km of Los Angeles since 1933, with stress change calculated at a depth of 10 km.

extended the method to consider the stress changes accompanying thrust earthquakes. We first calculate the optimally oriented vertical strike-slip and dipping thrust faults. We then resolve the earthquake-induced Coulomb stress on these planes and find the stress change that most promotes failure (12).

We calculate that the 1933 $M = 6.4$ Long Beach (13) and 1952 $M = 7.3$ Kern County (14) shocks raised the Coulomb stress at the site of the future San Fernando and Northridge shocks by at least 0.1 bar. The 0.1- to 0.2-bar stress changes shown in Fig. 2A are for an elastic half-space and thus do not include the effects of post-seismic asthenospheric relaxation during the two to six decades following the 1933 and 1952 earthquakes. The stress in the seismogenic crust must rise as the asthenosphere relaxes after the earthquakes. Complete relaxation of the asthenosphere, simulated by replacing the halfspace with a faulted 12.5-km-thick plate overlying an inviscid fluid, would yield a 0.8-bar stress rise at San Fernando and a 0.9-bar rise at Northridge.

Our calculations reveal that the 1971 San Fernando earthquake raised the Coulomb stress an additional 2 bars at the site of the future Northridge earthquake and 0.5 bar at the site of the future 1987 $M = 6.0$ Whittier Narrows shock (Fig. 2B). In both cases, the stress change was greatest on strike-slip faults, even though the 1987 and 1994 earthquakes were largely thrust events (15). A band of 1971 aftershocks extended to the future 1994 rupture zone (Fig. 1), and aftershocks in this band became more concentrated during the next 5 years (Fig. 2B). Aftershocks also spread to the future Whittier Narrows rupture zone. Seismicity filled most of the lobes where stress is calculated to have risen by >0.3 bar and was nearly absent where the stress is calculated to have dropped by >0.5 bar (Fig. 2B). During the 5- or 10-year period before the San Fernando earthquake, seismicity was nearly absent in the lobes that extended to the future Northridge and Whittier Narrows ruptures, reinforcing the deduction that the San Fernando earthquake stress changes triggered the

small shocks (16). The association of San Fernando aftershocks with regions of Coulomb stress rise is also evident in cross section (Fig. 3A). San Fernando aftershocks locate near the shallow part of the future Northridge rupture, where stress changes favor strike-slip or oblique failure.

Most of the aftershocks of the 1994 Northridge earthquake occurred in regions where the stress is calculated to have increased by >0.3 bar as a result of the fault slip; few aftershocks occurred where the stress is calculated to have dropped (Fig. 2C). The rate of occurrence of $1 \leq M \leq 2$ shocks appears to have climbed in metropolitan Los Angeles, 30 km southeast of the main shock, where the stress is calculated to have risen. The diffuse distribution of aftershocks above and up-dip of the thrust fault (Fig. 3B) is explained by the Coulomb stress increases associated with blind fault slip (17). Some 11 hours after the main shock, the Northridge aftershock zone expanded abruptly 6 km westward with a $M = 6$ aftershock (18) in an area where the calculated rise in Coulomb stress caused by the initial rupture was 0.75 bars (Figs. 2C and 3C). Surface faulting, cracking, and concentrated surface deformation were found at several sites after the Northridge earthquake (Fig. 1), and these contributed significantly to the earthquake damage (19). The calculated increases in Coulomb stress at these sites are large (Fig. 3, B and C), suggesting that the ground disturbance was the product of the off-fault changes in stress or strain in the compliant surface sediments. Thus, the location of the recorded $1 \leq M \leq 6$ aftershocks and surface faulting in the Northridge sequence is consistent with a model of stress triggering by the initial earthquake rupture.

The cumulative effect of all $M \geq 6$ earthquakes near Los Angeles since 1933 (Table 1) is calculated to be a decrease in

Fig. 3. Cross-sections of Coulomb stress changes on optimally oriented faults, shown with $M \geq 2$ aftershocks located within 4 km of the section lines shown in Fig. 1. Sites of surface faulting are keyed in Fig. 1. (A) Stress changes calculated for the San Fernando earthquake on optimally oriented strike-slip or thrust faults along a section connecting the 1971 and 1994 main shocks. Focal mechanisms of these aftershocks are largely strike-slip (3). (B) Section through the center of the Northridge aftershock sequence showing stress changes on optimally oriented thrust faults, because thrust focal mechanisms predominate. (C) Stress changes on optimally oriented thrust faults along a section through the center of the largest ($M = 6$) aftershock, 10 km west of the Northridge main shock.

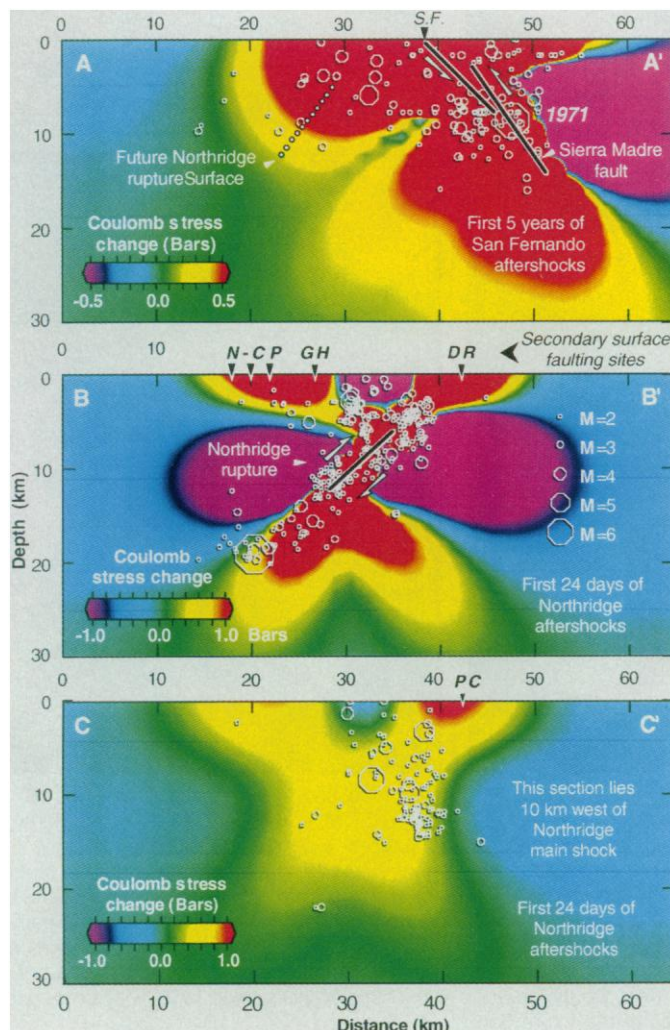


Table 1. The $M \geq 6$ earthquakes within 125 km of Los Angeles since 1933.

Earthquake	Date	M	Reference
Long Beach	10 Mar 1933	6.4	(13)
Kern County	21 Jul 1952	7.3	(14)
San Fernando	9 Feb 1971	6.7	(2)
Whittier Narrows	1 Oct 1987	6.0	(28)
Joshua Tree	23 Apr 1992	6.1	(29)
Landers	28 Jun 1992	7.4	(30)
Big Bear	28 Jun 1992	6.6	(31)
Northridge	17 Jan 1994	6.7	(4, 32)
Northridge aftershock	17 Jan 1994	6.0	(18)

Coulomb stress throughout a zone extending from the San Fernando Valley south to the coast (Fig. 2D). Stress also diminished by ~ 1 bar along the San Andreas fault between Tejon Pass and Palmdale, although the secular or steady stress accumulation of about 0.1 bar/year on the San Andreas fault from 1952 to 1994 likely erased the calculated stress drop there (20). A broad region in which stress is calculated to have risen by >1 bar encompasses the central Los Angeles basin and areas west of Northridge. We calculate that the eastern Oak Ridge fault, the eastern Santa Monica Mountains and western Elysian Park blind thrust faults, the central Sierra Madre fault, and the central Newport-Inglewood fault have all been subjected to stress increases of >1 bar (Fig. 2D; these faults are labeled in Fig. 1).

The stress rises we report could trigger events if a region or fault was within a few bars of failure before the triggering earthquake struck. Although a 1-bar Coulomb stress change is 50 to 100 times the tidal stress changes (21, 22), it is only 1 to 10% of the typical shear stress drop $\Delta\tau$ of an earthquake, so the stress increases we calculate are alone insufficient to cause earthquakes of any size (23). Likely stress accumulation rates in the greater Los Angeles area are about 0.1 bar/year or less, on the basis of the measured strain rate (20), so a 1-bar stress change corresponds to more than a decade of secular stress build-up. Thus, if faults fail when the Coulomb stress on a segment exceeds the failure threshold, then the 1933 and 1952 events advanced the occurrence of the San Fernando earthquake by about a decade, and the 1971 earthquake advanced the 1994 shock by a few decades. If, however, the Coulomb stress changes trigger small earthquakes or creep that cascade into widespread failure (24), then earthquake triggering may not require that a broad region has reached its failure threshold (25).

We interpret the close correspondence of the main shocks and their aftershocks to the modeled stress changes to imply that the sequence of large earthquakes since 1933 is, at least in part, a consequence of the static stress changes (26). This correspondence would not be possible unless some portions of the seismogenic crust in southern California were currently close to failure. Because we do not know precisely how close the major faults are to failure, our results cannot be used to predict the timing of large earthquakes. Instead, we suggest that these calculations describe where the earthquake potential in the greater Los Angeles region has risen and where it has dropped.

REFERENCES AND NOTES

1. T. L. Davis, J. Namson, R. F. Yerkes, *J. Geophys. Res.* **94**, 9644 (1989); R. S. Stein and R. S. Yeats, *Sci. Am.* **260**, 48 (June 1989).
2. T. H. Heaton, *Bull. Seismol. Soc. Am.* **72**, 2037 (1982). We simulated the variable slip model by four patches of slip on the San Fernando fault and five slip patches on the Sierra Madre fault.
3. J. H. Whitcomb, C. R. Allen, J. D. Garmany, J. A. Hileman, *Rev. Geophys.* **11**, 693 (1973).
4. E. Hauksson, K. Hutton, H. Kanamori, L. Jones, J. Mori, *Abstr. Annu. Meet. Seismol. Soc. Am.* **89**, 4 (1994).
5. A ~ 3000 -year repeat time for the Northridge earthquake fault is estimated by dividing the 3.5-m coseismic slip of K. W. Hudnut *et al.* (27) by the ~ 1 -mm/year fault slip rate argued by R. S. Yeats (in preparation). R. Crook Jr., C. R. Allen, B. Kamb, C. M. Payne, and R. J. Payne [*U.S. Geol. Surv. Prof. Pap.* **1339**, 27 (1987)] suggest a several-thousand-year repeat time for the western Sierra Madre fault, on which part of the San Fernando earthquake occurred, although M. Bonilla [*San Fernando, California, Earthquake of 9 February 1971*, L. M. Murphy, Ed. (National Oceanic and Atmospheric Administration, Washington, DC, 1973), vol. 3, p. 174] found a previous event 100 to 300 years old on a subsidiary strand of the San Fernando fault.
6. We used an elastic halfspace and let Young's modulus $E = 8.0 \times 10^{10}$ bars and Poisson's ratio $\nu = 0.25$, so the shear modulus $G = 3.2 \times 10^{10}$ bars. Very close to the slipped fault, the Coulomb stress change depends on the unknown details of the fault slip. Thus, stress changes calculated within a few kilometers of the earthquake sources are not meaningful. In contrast, stress changes far from the fault do not depend on the detailed slip function and are thus most diagnostic.
7. R. S. Stein and M. Lisowski, *J. Geophys. Res.* **88**, 6477 (1983); R. A. Harris and R. W. Simpson, *Nature* **360**, 251 (1992); S. C. Jaumé and L. R. Sykes, *Science* **258**, 1325 (1992).
8. P. A. Reasenberg and R. W. Simpson, *Science* **255**, 1687 (1992).
9. R. S. Stein, G. C. P. King, J. Lin, *ibid.* **258**, 1328 (1992).
10. The optimally oriented planes depend on the orientation and magnitude of the regional deviatoric compressive stress σ' , the stress change caused by the earthquake, and the coefficient of friction μ . In practice, results are insensitive to the magnitude of the regional stress as long as it is larger than the earthquake stress drop $\Delta\tau$; here we let $\sigma' = 100$ bars. Results are modestly sensitive to the assumed friction coefficient, which can range between 0 and 0.75, with lower μ corresponding to higher fluid pressure. Because we have little independent evidence to assign μ , we adopt a mid-range value of 0.4. A detailed sensitivity analysis is presented in (71).
11. G. C. P. King, R. S. Stein, J. Lin, *Bull. Seismol. Soc. Am.* **84**, 935 (1994).
12. The Coulomb stress change on optimally oriented faults is sensitive to the orientation of the regional tectonic stress field. Inversion of small-earthquake focal mechanisms and 1971–1988 aftershock sequences in the greater Los Angeles region [J. W. Gephart and D. W. Forsyth, *J. Geophys. Res.* **89**, 9305 (1984); L. M. Jones, *ibid.* **93**, 8869 (1988); E. Hauksson, *ibid.* **95**, 15365 (1990); _____ and L. M. Jones, *ibid.* **96**, 8143 (1991)] yields consistent values for the principal compressional axis of $N0^\circ$ to $N12^\circ E$ from the San Andreas fault south to Los Angeles, and $N10^\circ E$ to $N32^\circ E$ from south Los Angeles to Newport. Borehole breakouts of 10 oil wells in the Los Angeles and northeastern Ventura basin axis [V. S. Mount and J. Suppe, *J. Geophys. Res.* **97**, 11995 (1992)] furnish a $N21^\circ E$ compression. Here we use $N16^\circ E$, an average of these measurements.
13. E. Hauksson and S. Gross, *Bull. Seismol. Soc. Am.* **81**, 81 (1991). We simulated the seismic moment magnitude (M_0) = 6×10^{25} dyne-cm earthquake by a 23-km-long, $80^\circ N$ -dipping oblique fault with tapered slip at a depth of 2 to 17 km extending between the main shock and the largest aftershock.
14. R. S. Stein and W. Thatcher, *J. Geophys. Res.* **86**, 4913 (1981).
15. We use $\mu = 0.4$ and a $N16^\circ E$ regional stress direction. Calculated stress increases at the future Whittier Narrows and Northridge sites are twice as high for $\mu = 0.75$ than for $\mu = 0.0$. A $N6^\circ E$ direction favors failure at the Northridge earthquake site more than at Whittier Narrows; a $N26^\circ E$ direction favors rupture at Whittier Narrows more than at Northridge.
16. No corresponding seismicity rate declines are seen after the 1971 earthquake, perhaps because rate decreases are harder to detect, as described in (8).
17. On the basis of preliminary seismic [D. J. Wald and T. H. Heaton, *U.S. Geol. Surv. Open-File Rep.* **94-278** (1994); (18)] and geodetic (27) evidence, coseismic fault slip stops 6 to 8 km below the ground surface.
18. D. S. Dreger *et al.*, *Abstr. Annu. Meet. Seismol. Soc. Am.* **89**, 11 (1994).
19. D. Ponti *et al.*, *ibid.*, p. 31.
20. M. Lisowski, J. C. Savage, and W. H. Prescott [*J. Geophys. Res.* **96**, 8369 (1991)] measured a maximum shear strain rate in the Transverse Ranges northwest and northeast of Los Angeles to be about $0.13 \mu\text{strain}/\text{year}$, which yields a shear stress rate of 0.08 bars/year, with a higher value closer to the San Andreas fault. The principal compression rate is also about 0.08 bar/year.
21. A typical earthquake shear stress drop is 10 to 100 bars.
22. D. P. Hill *et al.*, *Science* **260**, 1617 (1993).
23. R. E. Abercrombie [*Proceedings of the 11th International Symposium on the Observation of the Continental Crust Through Drilling*, Santa Fe, NM, 25 to 30 April 1994, p. 221] found that the 10- to 100-bar static stress drops $\Delta\tau$ of $M \geq -1$ earthquakes recorded in the Cajon Pass borehole are indistinguishable from those of larger shocks. Thus, there is no evidence that the ~ 1 -bar stress changes we report can cause microearthquakes unless the faults are already close to failure.
24. R. Abercrombie and J. Mori [*Bull. Seismol. Soc. Am.* **84**, 725 (1994)] advance such a case for the Landers earthquake.
25. This could occur because the stress change occurs at a fault asperity or because the system as a whole is in a state of self-organized criticality [see, for example, P. A. Cowie, C. Vabbeste, D. Sor-nette, *J. Geophys. Res.* **98**, 21809 (1993)].
26. It is also possible that the dynamic stresses play a role in earthquake triggering. Hill *et al.* (22) and J. G. Anderson *et al.* [*Bull. Seismol. Soc. Am.* **84**, 863 (1994)] argue that distant aftershocks of the Landers earthquake were triggered by dynamic strains associated with the Landers rupture. P. Spudich, L. K. Steck, M. Hellweg, J. B. Fletcher, and L. M. Baker [*J. Geophys. Res.*, in press] suggest that at the site of the Big Bear event, the dynamic stresses are 3 to 6 times larger than the static stress changes, but they persist for <20 s and do not have lobes of stress decrease.
27. K. W. Hudnut *et al.*, *Abstr. Annu. Meet. Seismol. Soc. Am.* **89**, 40 (1994).
28. J. Lin and R. S. Stein, *J. Geophys. Res.* **94**, 9614 (1989).
29. E. Hauksson, L. M. Jones, K. Hutton, D. Eberhart-Phillips, *ibid.* **98**, 19835 (1993).
30. D. J. Wald and T. H. Heaton, *Bull. Seismol. Soc. Am.* **84**, 668 (1994).
31. L. E. Jones, S. E. Hough, D. V. Helmbarger, *Geophys. Res. Lett.* **20**, 1907 (1993).
32. Parameters are $41.6^\circ S$ dip, 5.84-km burial depth, 10.3-km down-dip width, 8.1-km length, 100° strike, 3.52-m uniform slip, and $M_0 = 0.9 \times 10^{26}$ dyne-cm. This model, based on geodetic observations, likely illuminates the fault patch with greatest slip but underestimates the fault area. See (27).
33. We thank R. W. Simpson, for discussion and extensive calibration of our respective programs, and M. H. Murray, for sharing his preliminary geodetic models of the Northridge earthquake. We also thank W. Thatcher, J. Savage, T. Heaton, P. Reasenberg, and two anonymous referees for thoughtful reviews. We are grateful for the financial and scientific support of the Southern California Earthquake Center.

22 April 1994; accepted 26 July 1994